AD-A039 187 VARIAN ASSOCIATES PALO ALTO CALIF F/G 9/1
IMPROVED DUAL-MODE ELECTRON GUN.(U)
MAR 77 F BJORNSTAD F30602-76-C-0177
UNCLASSIFIED RADC-TR-77-95 NL

1 OF 1
ADA039187

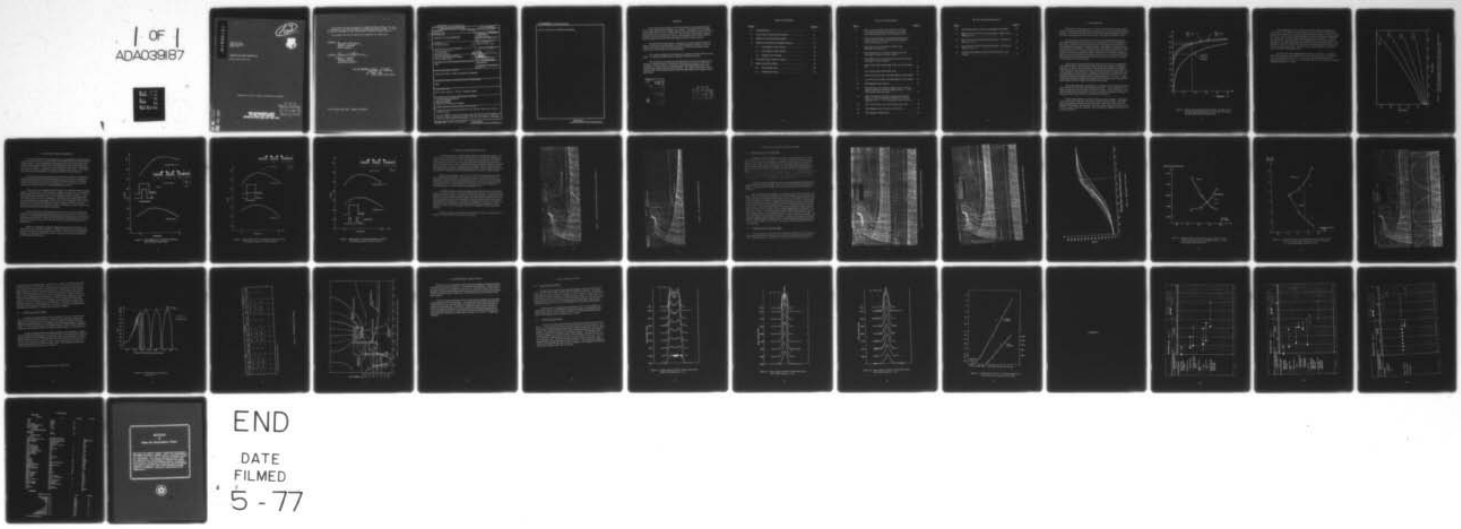

END

DATE
FILMED
5-77

12

B. S.

RADC-TR-77-95
Technical Report
March 1977

IMPROVED DUAL-MODE ELECTRON GUN

Varian Associates, Inc.

Approved for public release; distribution unlimited.

ROME AIR DEVELOPMENT CENTER
AIR FORCE SYSTEMS COMMAND
GRIFFISS AIR FORCE BASE, NEW YORK 13441

This report has been reviewed by the RADC Information Office (OI) and is releasable to the National Technical Information Service (NTIS). At NTIS it will be releasable to the general public including foreign nations.

This report has been reviewed and is approved for publication.

APPROVED: Ronald W. Vandivier
RONALD W. VANDIVIER
Project Engineer

APPROVED: Joseph L. Ryerson
JOSEPH L. RYERSON
Technical Director
Surveillance Division

FOR THE COMMANDER: John P. Huss
JOHN P. HUSS
Acting Chief, Plans Office

Do not return this copy. Retain or destroy.

UNCLASSIFIED
SECURITY CLASSIFICATION OF THIS PAGE (When Data Entered)

(19) REPORT DOCUMENTATION PAGE	READ INSTRUCTIONS BEFORE COMPLETING FORM
1. REPORT NUMBER (18) RADC-TR-77-95	2. GOVT ACCESSION NO. (9) Technical rept.	3. RECIPIENT'S CATALOG NUMBER
4. TITLE (and Subtitle) (6) IMPROVED DUAL-MODE ELECTRON GUN,	5. TYPE OF REPORT & PERIOD COVERED Interim Report Apr 76 — Dec 76,
	6. PERFORMING ORG. REPORT NUMBER N/A
7. AUTHOR(s) (10) Fredrik Bjornstad	8. CONTRACT OR GRANT NUMBER(s) (15) F30602-76-C-0177 New
9. PERFORMING ORGANIZATION NAME AND ADDRESS Varian Associates, Inc. 611 Hansen Way Palo Alto CA 94303 (16)	10. PROGRAM ELEMENT, PROJECT, TASK AREA & WORK UNIT NUMBERS 62702F (17) 02 55730201
11. CONTROLLING OFFICE NAME AND ADDRESS (11) Rome Air Development Center (OCTE) Griffiss AFB NY 13441	12. REPORT DATE Mar 1977
	13. NUMBER OF PAGES (12) 41 p.
14. MONITORING AGENCY NAME & ADDRESS(if different from Controlling Office) Same	15. SECURITY CLASS. (of this report) UNCLASSIFIED
	15a. DECLASSIFICATION/DOWNGRADING SCHEDULE N/A

16. DISTRIBUTION STATEMENT (of this Report)

Approved for public release; distribution unlimited.

17. DISTRIBUTION STATEMENT (of the abstract entered in Block 20, if different from Report)

Same

18. SUPPLEMENTARY NOTES

RADC Project Engineer: Ronald W. Vandivier (OCTE)

19. KEY WORDS (Continue on reverse side if necessary and identify by block number)

Non-intercepting gridded gun
Dual mode operation
Rotational energy
Magnetic flux threading of cathode

20. ABSTRACT (Continue on reverse side if necessary and identify by block number)

An advanced non-intercepting gridded gun was designed, fabricated, and preliminary tested.

The use of magnetic flux in the cathode region preserves the beam diameter when the grid voltage is reduced for a lower power mode of operation. This will result in a more stable TWT performance, since the gain difference associated → next page

DD FORM 1 JAN 73 1473 EDITION OF 1 NOV 68 IS OBSOLETE

UNCLASSIFIED
SECURITY CLASSIFICATION OF THIS PAGE (When Data Entered

364100 Issued

with the two modes is significantly reduced.

SUMMARY

The design approach chosen for the electron guns in this study involves the use of partial magnetic flux threading of the cathode. The magnetic flux threading of the cathode allows the use of higher magnetic focusing field and preserves the beam diameter between two modes of operation. The rms value of the periodic magnetic focusing field had to be limited to 1.35 times the Brillouin value to avoid excess rotational energy of electrons at the beam edge in the field reversal regions.

Two gun types are under study. One gun uses a single control grid and produces a solid beam in both the high and low current modes of operation. In the second gun, two control grids are used to produce a solid beam in the high current mode, and a hollow beam in the low current mode.

The computer design of the first gun and its magnetic focusing system is completed. An experimental gun has been evaluated in the beam analyzer.

The feasibility of producing and focusing the beam in the second gun has been proven by computer analyses. The details of the double grid system is still under evaluation. A hollow beam will initially be generated experimentally with a non-emissive button in the center part of the cathode. The stability of this beam will be explored under PPM focusing condition before the final design of the complex control grid system.

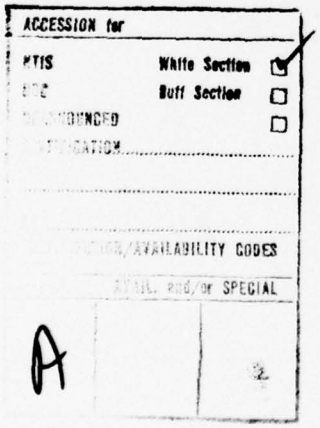

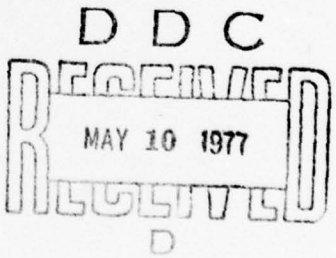

TABLE OF CONTENTS

LIST OF ILLUSTRATIONS

LIST OF ILLUSTRATIONS (Cont'd)

1. INTRODUCTION

The objective of this program is to develop, fabricate and evaluate an advanced non-intercepting gridded gun design for dual-mode traveling wave tube (TWT) application. The program is expected to demonstrate that the performance objectives have been achieved by testing the electron beam in an actual TWT under rf drive.

In a traveling wave tube, the beam voltage is determined by the required synchronization between the electrons and the electromagnetic wave propagation on the circuit. Changes in the beam power for dual-mode operation must therefore be accomplished by changes in the beam current. The changes in the beam current also affect gain and efficiency. The electrostatic beam diameter produced by a gridded gun will decrease as the grid voltage is decreased for lower beam current. A reduction in the beam diameter will cause a reduction in the interaction impedance. Since gain is proportional to the one-third power of the interaction impedance, this will accentuate the gain difference between the two modes of operation, in addition to the decrease in the beam current.

The design approach chosen for this study involves the use of magnetic flux in the cathode region. The electron trajectories will tend to follow the magnetic flux lines. It can be seen from Figure 1 that with partial magnetic flux threading of the cathode the beam diameter is better preserved in the lower power mode. For a current pulse-up ratio of 3:1 and a magnetic focusing field of 1.35 times the Brillouin field (B_{Br}) the ratio between mean diameters in the two modes is 0.89. It is desirable to keep the normalized average rotational energy to 0.1 or less. Figure 2 shows the restrictions placed on the amount of focusing field used to minimize the effect of high rotational energy in the field reversal region.

Two design approaches were chosen as a result of a small-signal gain analysis using different current density distributions in the beam. In one approach a solid beam is produced in the two modes of operation by using a single control grid. Magnetic flux threading of the cathode was used to minimize the reduction of the beam diameter between high- and low- current modes of operation.

In the second approach, two control grids are used to produce a solid beam in the high-current mode and a hollow beam in the low-current mode. The hollow beam is generated by elimination of current in the center core of the solid beam. Magnetic flux threading of the cathode will also be used for this gun in order to minimize the change of the outer diameter, and to prevent the collapse of the hollow low-current mode beam.

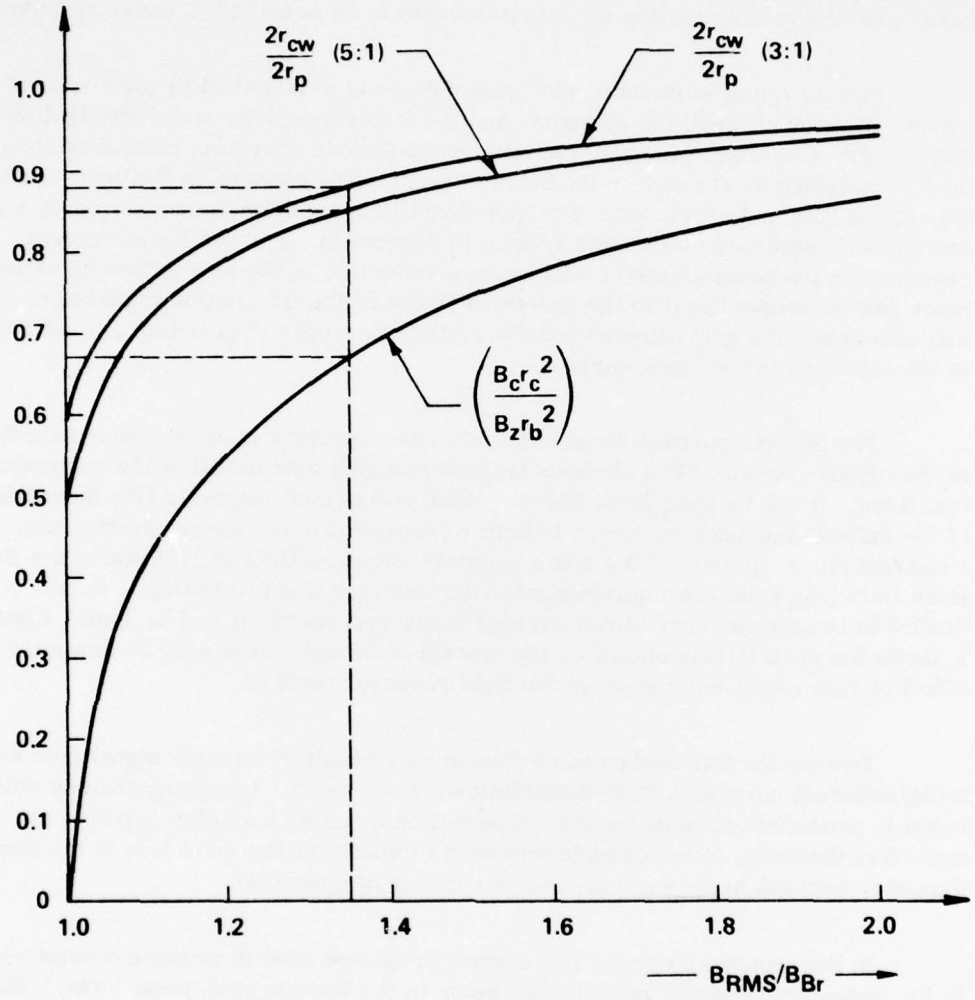

Figure 1. Relative Flux Threading of the Cathode, and Ratios of cw and Pulse Mode Beam Diameters vs the Ratio of the RMS Focusing Field and the Brillouin Field.

A gun producing the solid cw beam has been fabricated and evaluated in a beam analyzer. The hollow cw beam case has not yet been tested experimentally. A step-by-step approach was selected to better study the stability of the hollow beam. The hollow beam will first be generated with the simplest possible gun configuration. The complex grid structure will be substituted with a focus electrode to minimize beam distortion. The hollow beam will be obtained with a non-emissive button on the cathode. The initial test will be performed using a solenoid-focusing field. The stability and behavior of the hollow beam in a solenoid-focusing field is known from several existing electron guns. This test result will then establish a standard for comparision with PPM focused beams.

The hollow beam will subsequently be tested in a PPM field. The effect of high rotational energy in the field-reversal region will be studied. From Figure 2 it can be seen that the ratio of the rms focusing field and the Brillioun field (B_{rms}/B_{Br}) should not exceed 2.0 for a microperveance of 0.5 to obtain a normalized rotational energy of 0.1 or less.

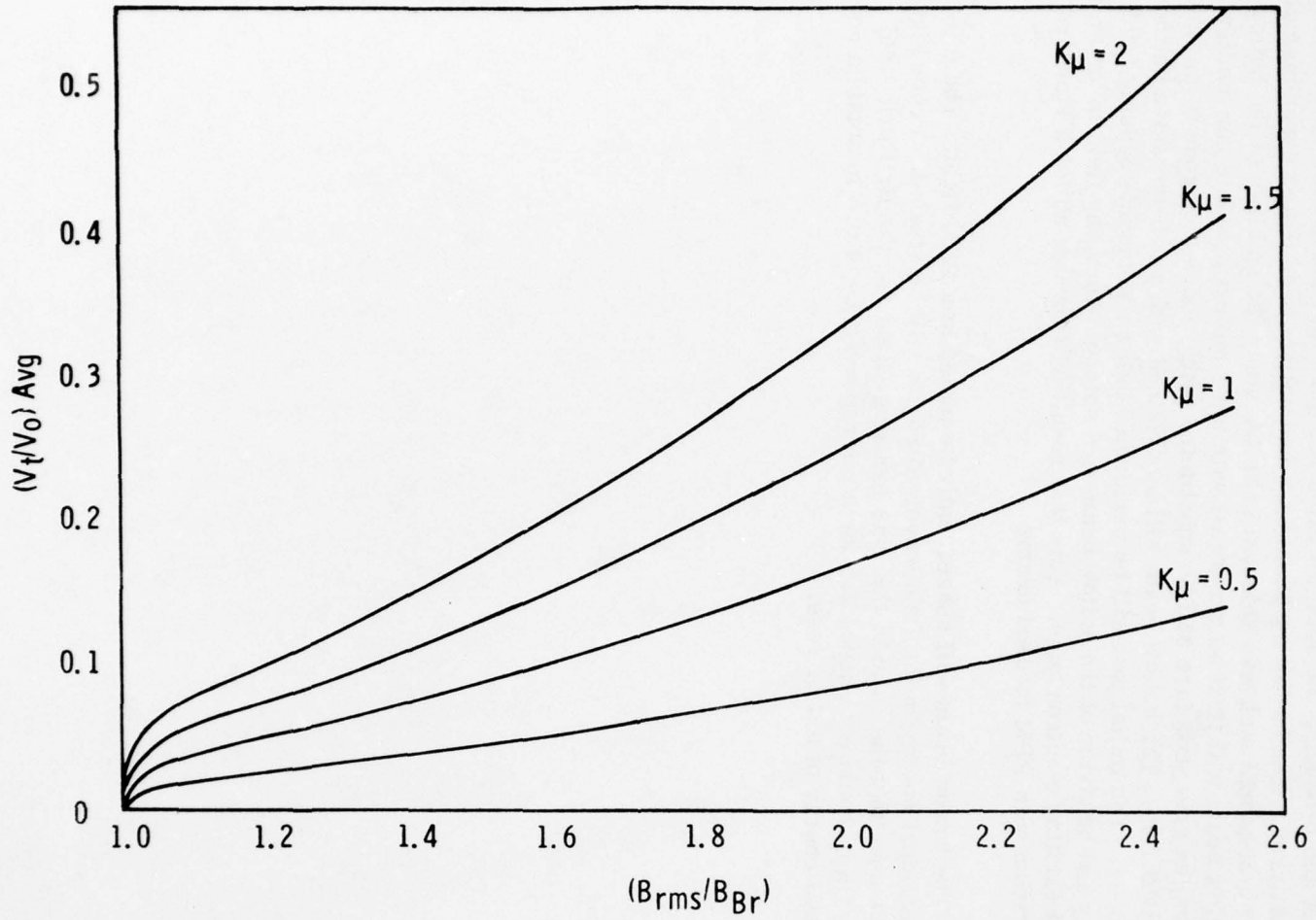

Figure 2. PPM Focused Solid Beam Normalized Average Energy of Edge Electrons vs the Ratio of the RMS Focusing Field and the Brillouin Field.

2. SELECTION OF BEAM PARAMETERS

In order to determine the helix parameters, a small-signal computer program was used which takes into account the effect on the space charge waves of flux threading the cathode. It was assumed that a nondispersive velocity characteristic could be obtained by suitably loading the helix with longitudinal vane segments attached to the inside of the barrel. From cold test data on similar circuits, it was determined how much the interaction impedance would be reduced by such loading. This reduction in the interaction impedance was taken into account in the calculations.

From several trials it was found that maximum gain flatness was obtained for a ratio of beam diameter to inside helix diameter of 0.6. It was also found that a uniform output helix would not give the required wideband efficiency, so the phase velocity was reduced near the end of the output helix. A 5 percent phase velocity step led to the most satisfactory small-signal gain performance.

Three cases were computed to show the effects of various approaches in beam design. First the case of no-flux through the cathode was analyzed. For comparison the computed small signal gain vs. frequency response is shown in Figure 3. Since the beam diameter varies by a factor of 1.7 between the low-current and high-current modes the change in gain is substantial. If the low-current mode gain were to be 30 dB minimum, the gain change would be about 52 dB at midband. The very high gains in the pulse mode would obviously result in stability problems, both from backward-wave oscillation and internal feedback. In addition, the gain variation over the band is about 20 dB in the high-current mode.

Next, if 67 percent of the magnetic flux in the beam is allowed to thread the cathode, the change in beam diameters between the low- and high- current modes is only 1.14. The small-signal gain characteristics are shown in Figure 4 for the case of both beams being solid. In this case, the difference in mid-band gain is 36 dB and the gain variation over the band is less than 13 dB, when the low current gain is 30 dB minimum.

Finally, a calculation was made considering the cw beam to be hollow. Results for this case are shown in Figure 5. Because of higher interaction impedance of the hollow beam, the gain change between modes is less than 25 dB, and the gain variation over the band is less than 11.5 dB. The gain is also nearly balanced at the band edges for both modes.

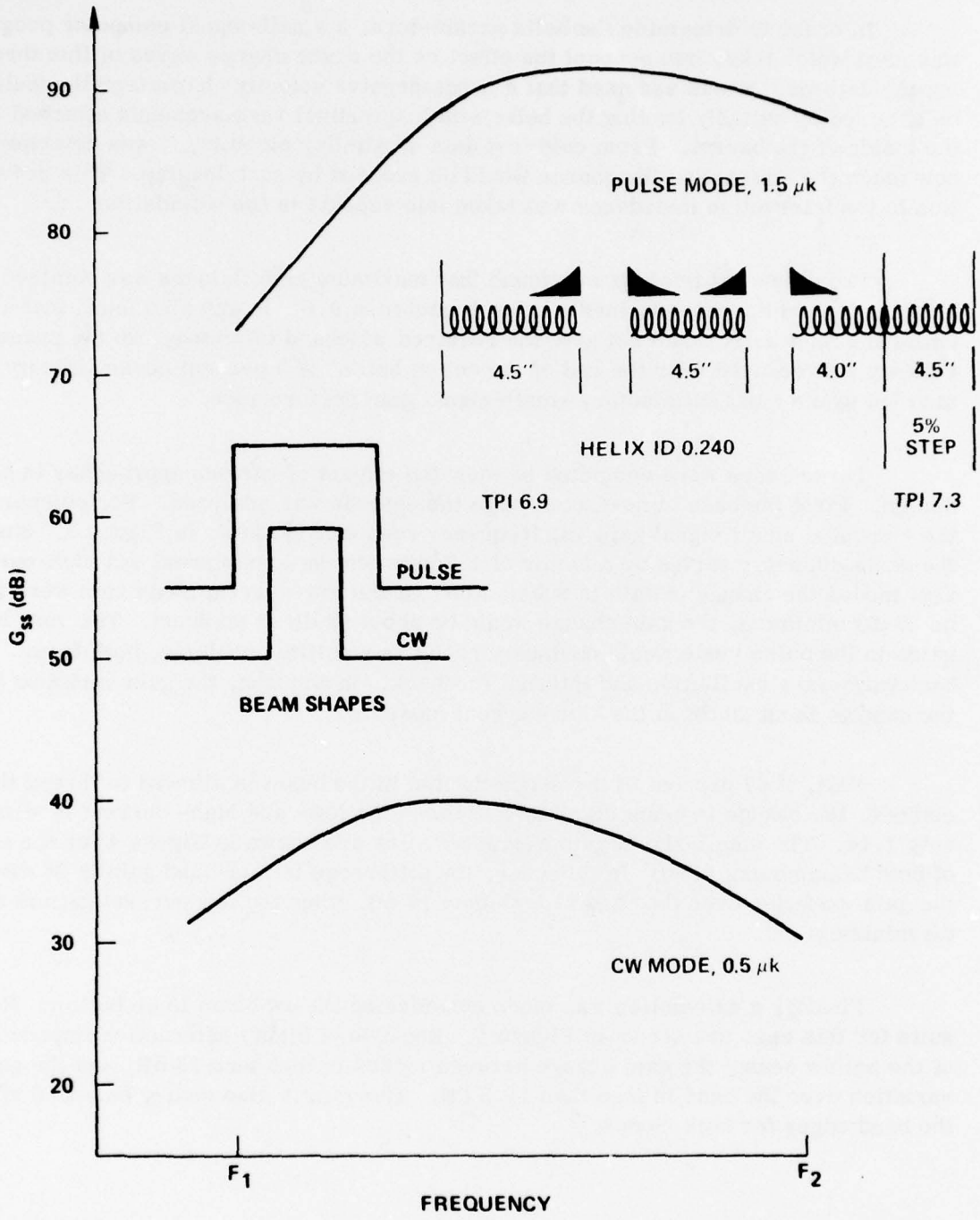

Figure 3. Small Signal Gain vs Frequency Response with Brillouin Focused Beams.

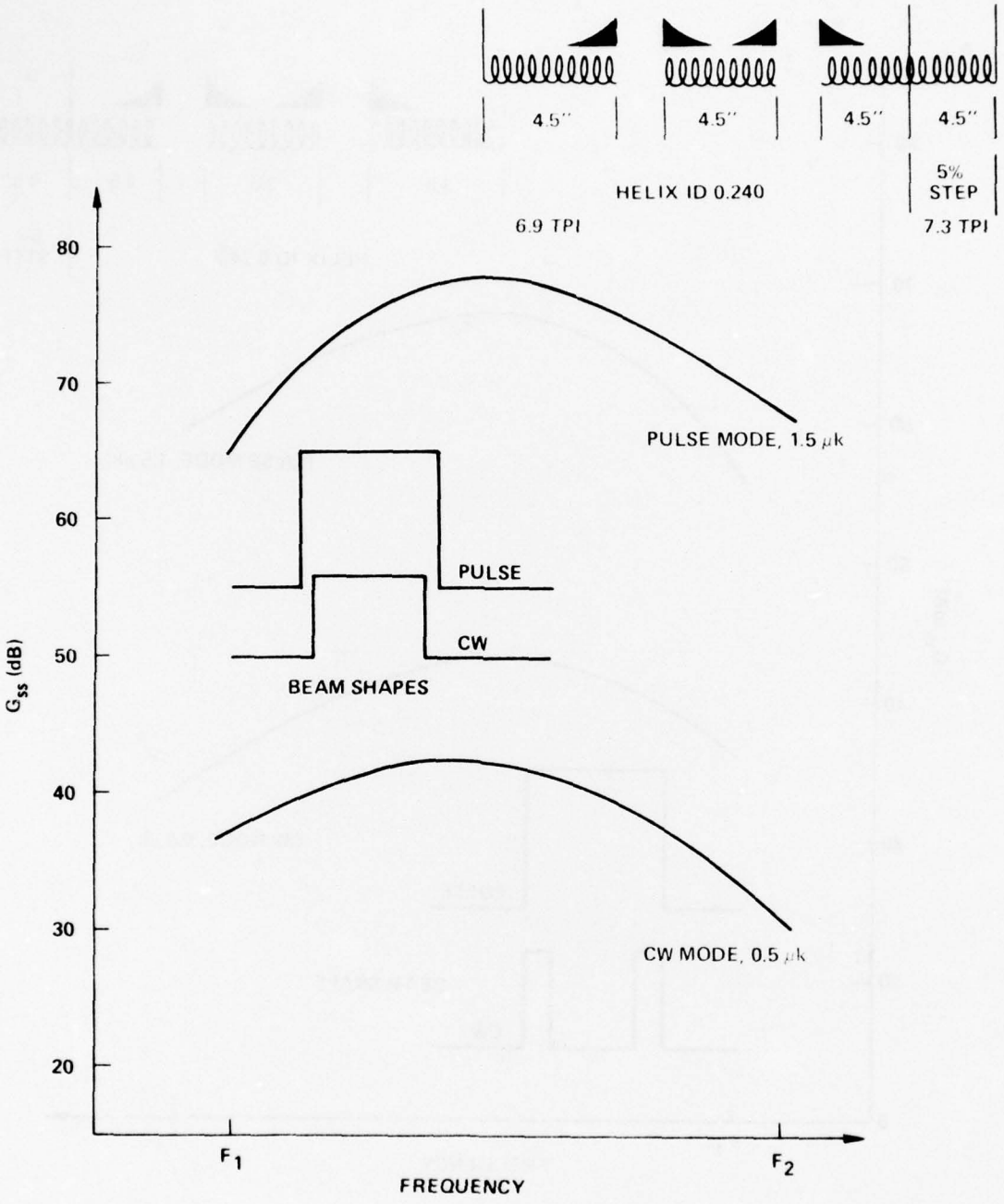

Figure 4. Small Signal Gain vs Frequency Response with Flux Threading of Cathode, cw Beam is Solid.

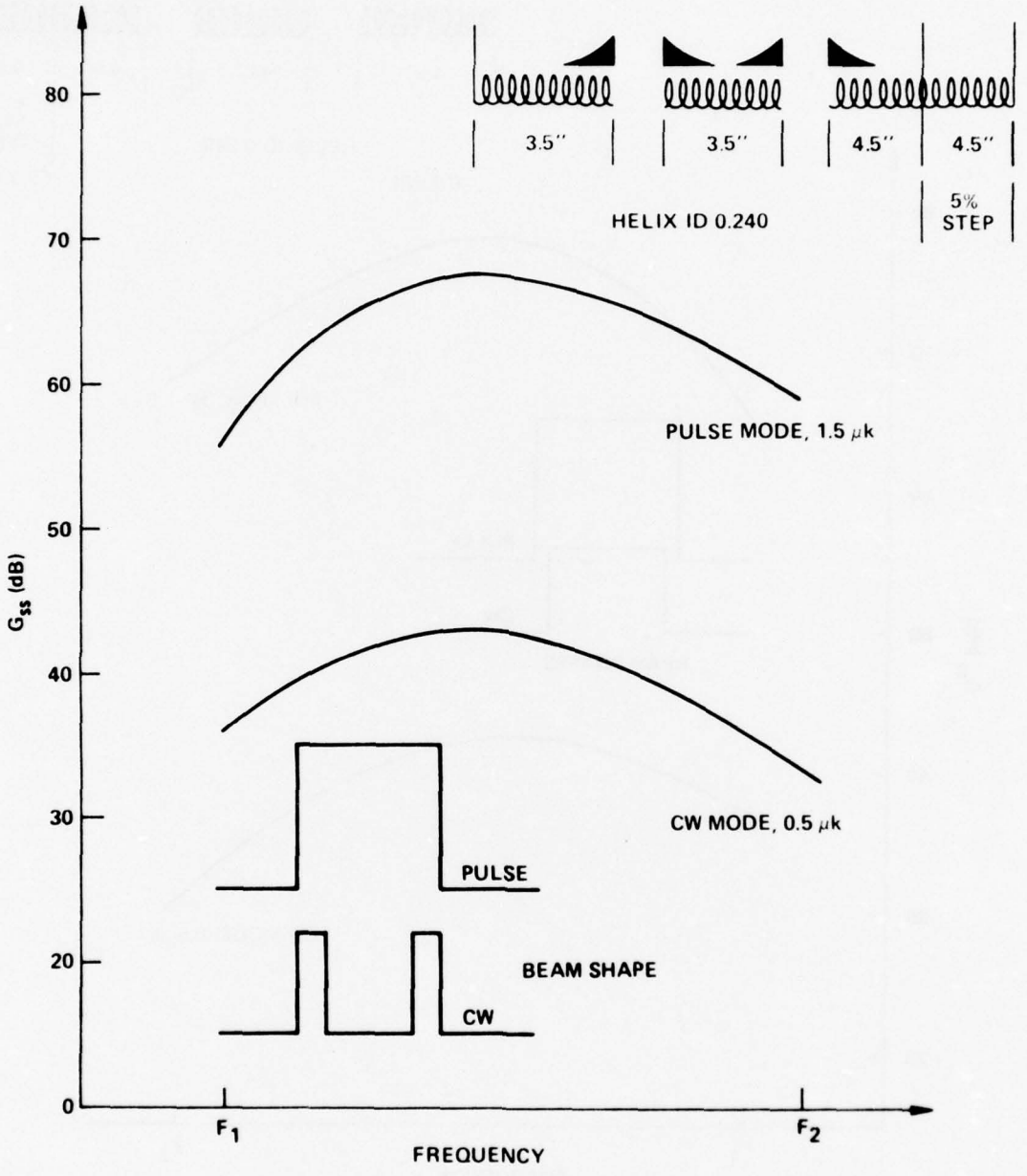

Figure 5. Small Signal vs Frequency Response with Flux Threading of Cathode cw Beam is Hollow.

3. DESIGN OF ELECTROSTATIC BEAM

A computer analysis was made using Varian's gun simulation program. For convenience in comparison of results the scale factor of the guns was such that the active cathode diameter was 1.0 in. The electron beam was injected with uniform current density into the plane of the control grid with the appropriate currents for the two operating modes. The 15 reference electrons used in the analysis are launched perpendicular to the grid. Distortion in beam optics produced within the individual grid cells is neglected in this preliminary analysis. The formation of the beamlets within the individual grid cells was the subject of a separate computer study.

Three area convergences of 4:1, 6.5:1, and 10:1 in the high-current mode were selected for this analysis. The radius of curvature of the control grid was adjusted for good laminarity in the high-current mode. When the area convergence of the gun increased, the separation increased between the beam minimums for the two operating modes. This separation will contribute to scalloping when the two operating beams are focused with the same magnetic field.

A detailed computer analysis was made to determine the proper grid cell geometry to minimize electron cross-over within the grid structure. Two control grids in addition to the focus grid are required, when the low-current mode beam is hollow. This case required a fairly extensive study. It showed that the formation of the beamlets within the grid cells is fairly sensitive to the grid thickness and to the spacing between the two control grids. In general, the smallest lens effect and the best optical performance is obtained for the smallest grid thickness and spacing. A grid thickness of .003 in. and a spacing of .005 in. was selected to assure mechanical rigidity.

When the beam was solid in the low-current mode, only one control grid was required. Beam distortion in this case was minimal.

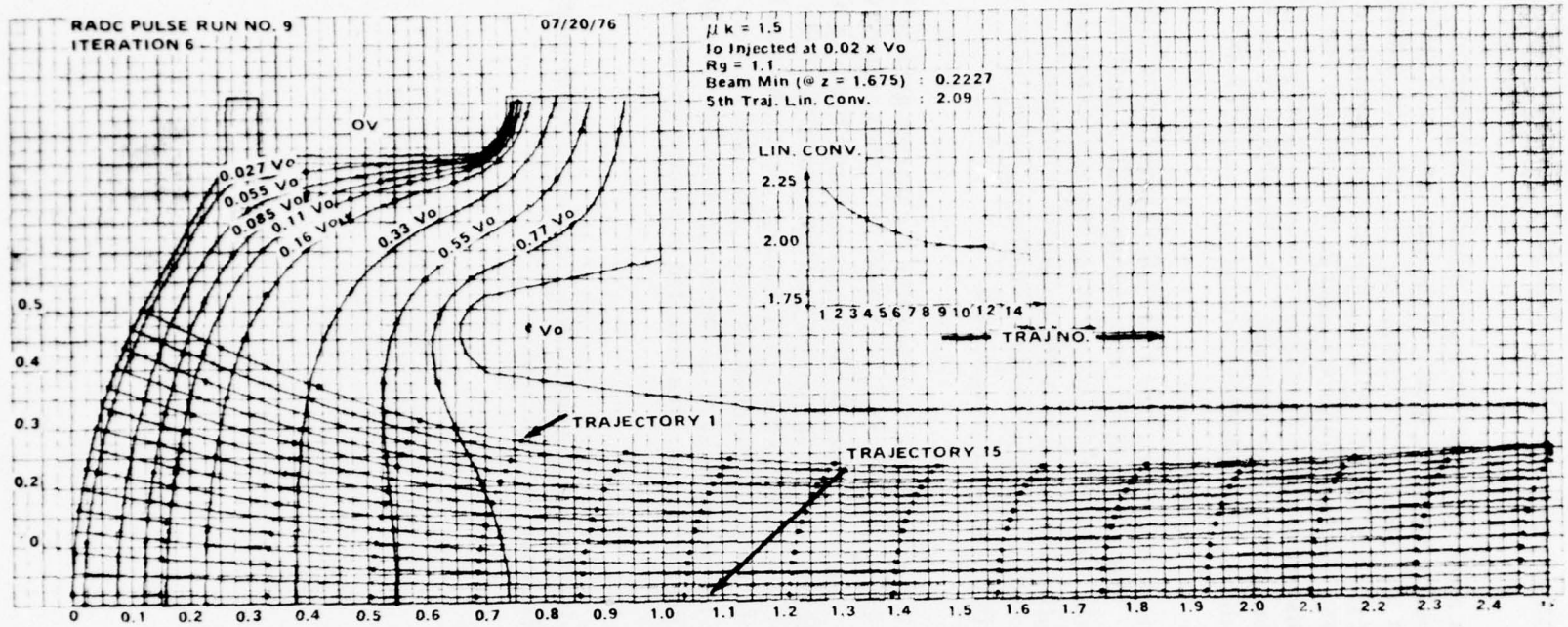

Figure 6. High-Current Mode Electrostatic Beam Area Convergence 4:1

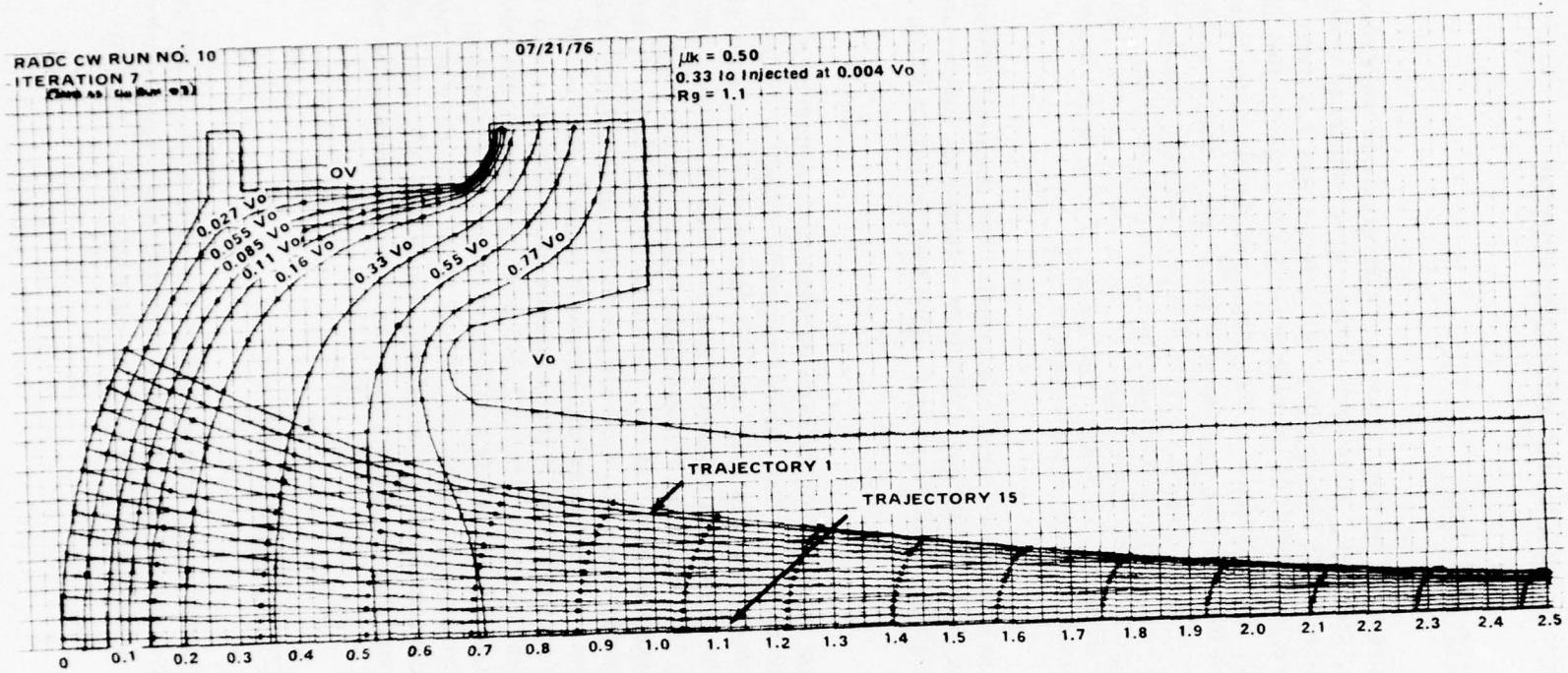

Figure 7. Low-Current Mode Electrostatic Beam.

4. DESIGN OF MAGNETIC FOCUSING SYSTEM

4.1 RMS MAGNETIC FIELD ANALYSIS

As mentioned in the previous section, three area convergences were chosen for this analysis, 4:1, 6.5:1, and 10:1. To ensure a normalized rotational energy level of 0.1 or less, the selected RMS focusing field of the beam was 1.3 times the Brillouin value. This requires that about 64 percent of the RMS magnetic flux in the beam threads the cathode. (See Figure 1.) The shaping of the magnetic field in the gun region was performed for minimal scalloping of the beam in the focusing region for the high-current mode. Figures 8 and 9 show computer simulations with magnetic field. Preservation of the beam diameter in the low-current mode due to magnetic flux threading of the cathode resulted in a ratio of the high- and low-current mode beam diameter of 0.89. The ratio of the beam diameters under Brillouin-focused condition was approximately 0.5.

As expected, the beam with the 4:1 area convergence had the least amount of scalloping in either operating mode. This beam was then selected for further investigation. The slope of the magnetic field in the gun region was varied as shown in Figure 10.

The electrostatic beam minimum of the high-current mode occurred at a distance 1.675 in. away from the cathode. The various magnetic slopes with their field value at this point are referenced in Figures 11 and 12. Maximum beam excursions for the two modes of operation vs percent magnetic field at 1.675 in. away from the cathode are plotted in Figure 11. When the two operating beams were focused with the same magnetic field, it was apparent that only one could be favored for optimum performance. The best magnetic slope would be one producing an equal maximum beam excursion of the two beams. This resultant magnetic slope is labeled "R" in Figure 10. Figure 12 is a plot of the ratio of the maximum beam diameters for the two operating modes vs percent magnetic field at 1.675 in away from the cathode. A larger maximum beam excursion corresponds to a larger amount of scalloping. The magnetic resultant-slope R produced 7 percent scalloping in the high-current mode and 22.5 percent in the low-current mode. A similar analysis was performed when the low-current mode beam was hollow. In this case the R-slope produced 10 percent scalloping.

4.2 PPM MAGNETIC FIELD ANALYSIS

A PPM magnetic field profile was constructed on the basis of the result in the RMS magnetic field study. The ratio of the plasma wavelength and magnet period was 3.1 for the high-current mode and 5.4 for the low-current mode, which are

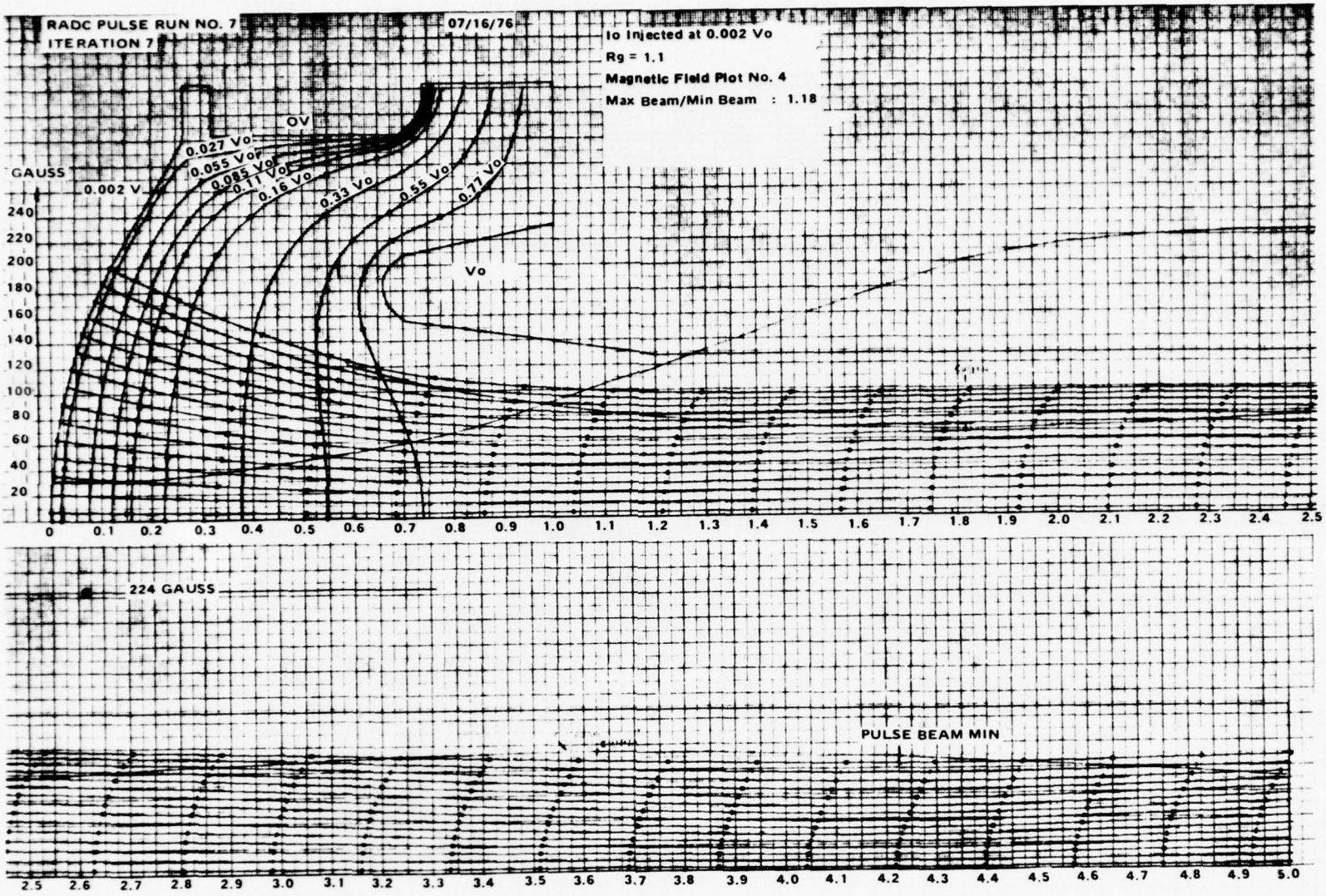

Figure 8. High-Current Mode Beam with RMS Magnetic Field Applied.

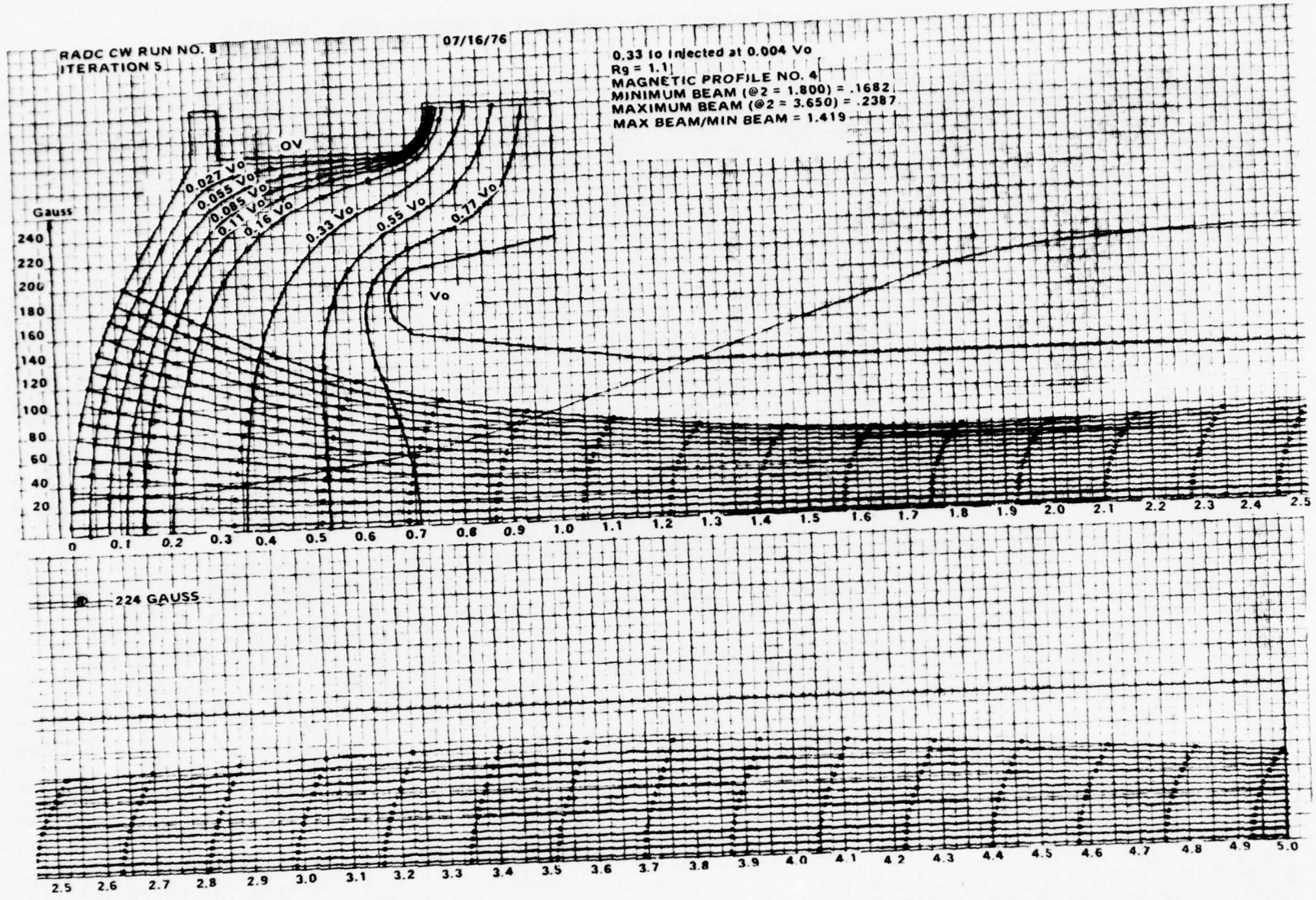

Figure 9. Low-Current Mode Beam with RMS Magnetic Field Applied.

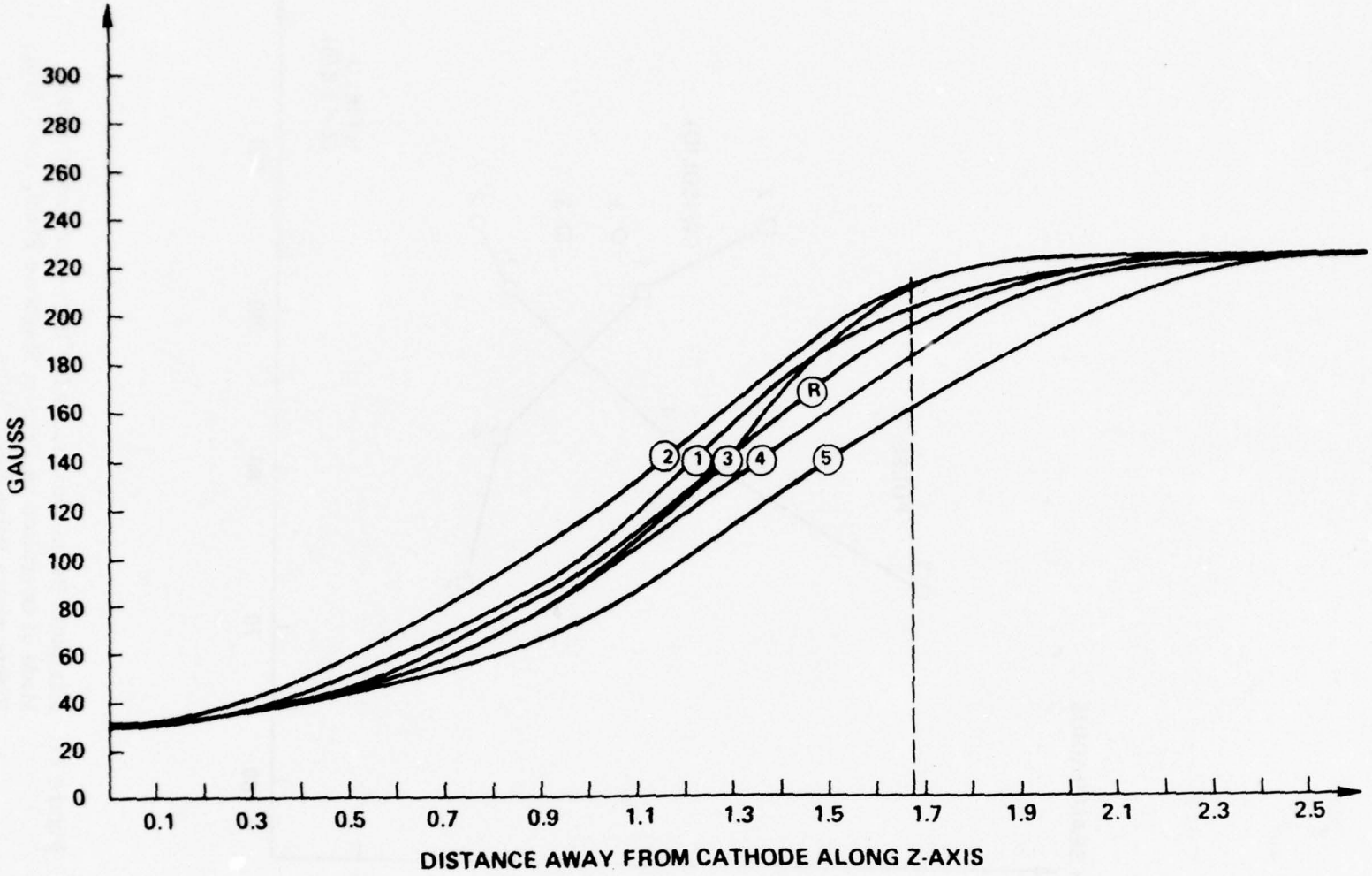

Figure 10. RMS Magnetic Field Profiles

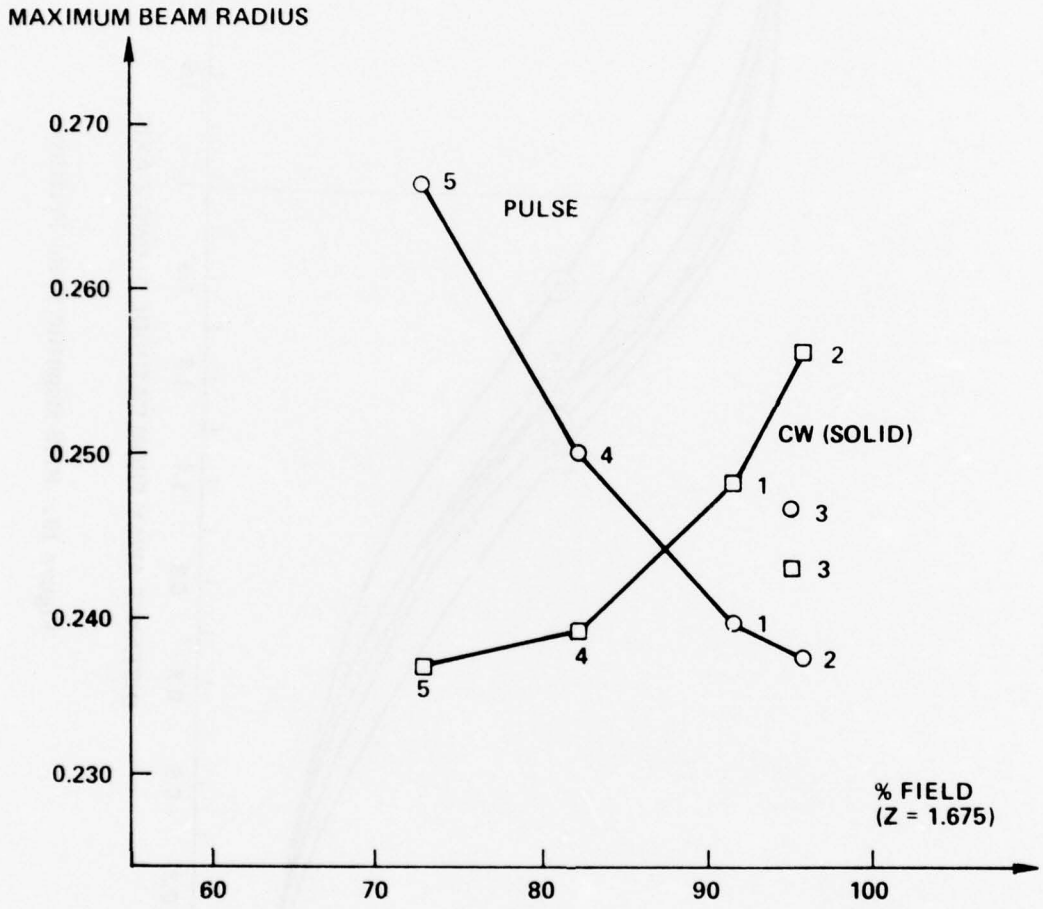

Figure 11. Maximum Beam Excursions for High- and Low-Current Mode of Operation vs Percent Magnetic Field, z = 1.675, Electrostatic Pulse Beam Min.

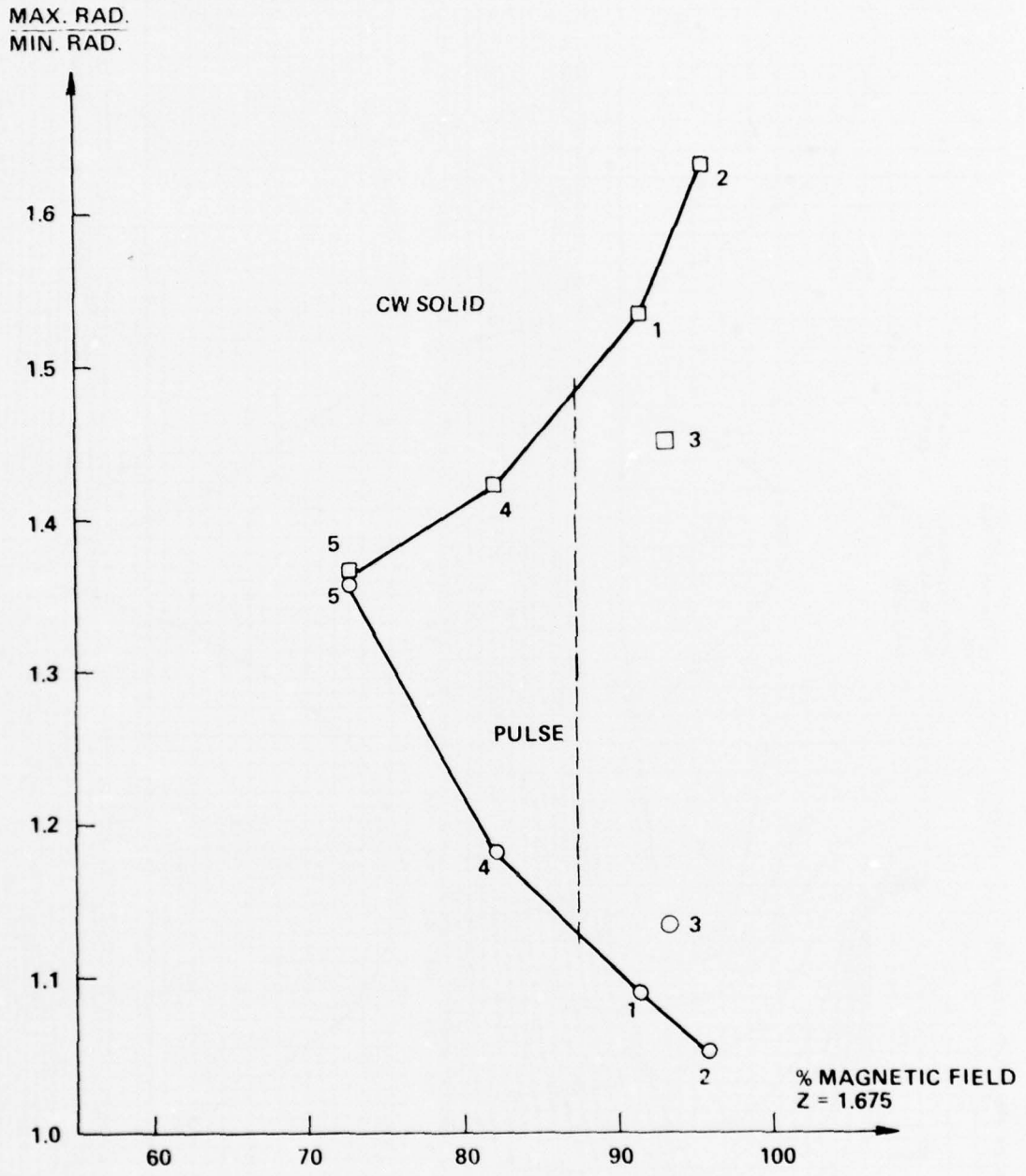

Figure 12. Ratios of Maximum and Minimum Beam Excursion for High- and Low-Current Mode of Operation vs Percent Magnetic z = 1.675 Electrostatic Pulse Beam Min.

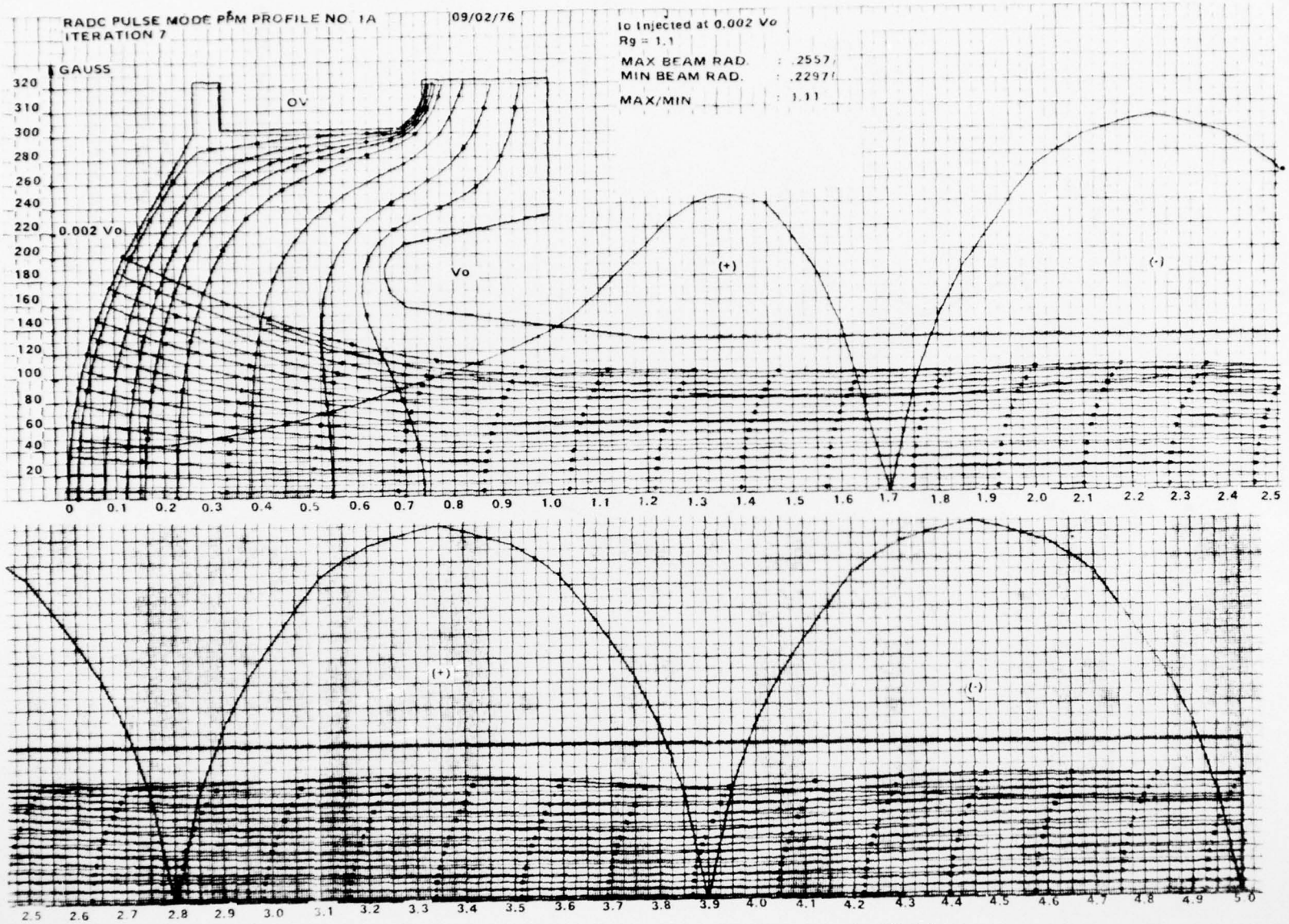

Figure 13. High-Current Mode Beam with PPM Magnetic Field.

acceptable values for good focusing. Figure 13 is a computer simulation of the high-current mode beam in a PPM field. Since the slope of the magnetic field in the gun area had been determined in the previous study, the only parameter varied was the length of the axial extension of the first half-period. The location of first magnetic field reversal with respect to the beam minimum of the high-current mode was located. The field shapes used for the computer simulation were plotted in Figure 14, with the corresponding results in Figure 15. The effect of the variation in the axial extension of the first half-period was minimal. The scalloping of the outer edge electrons was low in all three cases. The high-current mode had, according to the computer prediction, less than 6 percent scalloping. The solid low-current mode beam had 16 percent, and the hollow beam, 14 percent. The velocity spread between the outside and inside beam trajectory was also quite acceptable.

4.3 MAGNETIC CIRCUIT DESIGN

A computer program solving LaPlace's equation was used to design the magnetic circuit needed for the PPM field. The design of the individual magnets and polepieces was made in accordance with Sterret and Heffner; "Design of Periodic Magnet Focusing Structures".[1] The design of the PPM focusing system is shown in Figure 16. The large hole diameter in the gun polepiece and the radially magnetized magnet are the principal elements providing the flux threading of the cathode region.

An actual magnetic circuit was designed based on this information. Experiments to duplicate the PPM goal curve were performed. With some minor correction, the goal was very nearly duplicated and the slope of the magnetic field in the cathode region matched fairly well. The axial extension of the first half-period was approximately 0.1 in larger than originally planned. This magnetic field was used in the gun simulation program to confirm the beam shape. The scalloping of the beam in both high- and low current mode was acceptable.

1. IRE Transactions on electron devices, January 1958.

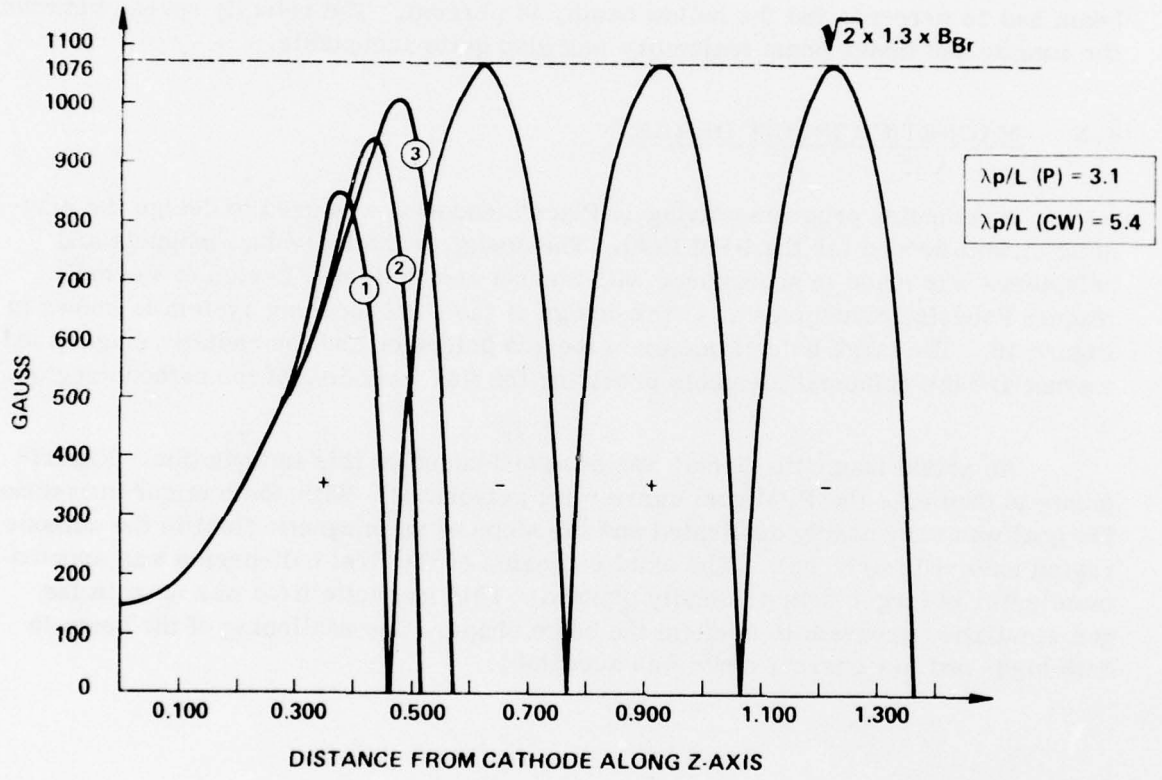

Figure 14. PPM Magnetic Field Profiles
Actual Values.

PPM PROFILE	PULSE				CW, SOLID				CW, HOLLOW			
	MAX BEAM RAD.	MIN BEAM RAD.	MAX/MIN	$\frac{V_{z(1)MAX} - V_{z(1)MIN}}{V_{z(1)MAX} + V_{z(1)MIN}}$*	MAX BEAM RAD.	MIN BEAM RAD.	MAX/MIN	$\frac{V_{z(1)MAX} - V_{z(1)MIN}}{V_{z(1)MAX} + V_{z(1)MIN}}$*	MAX BEAM RAD.	MIN BEAM RAD.	MAX/MIN	$\frac{V_{z(1)\,MAX} - V_{z(1)\,MIN}}{V_{z(1)\,MAX} + V_{z(1)\,MIN}}$*
I	0.2557	0.2297	1.11	0.13	0.2558	0.1917	1.33	0.12	0.2476	0.1931	1.28	0.12
II	0.2586	0.2313	1.12	0.13	0.2543	0.1929	1.32	0.12	0.2521	0.1934	1.30	0.12
III	0.2617	0.2300	1.14	0.12	0.2532	0.1936	1.31	0.12	0.2500	0.1933	1.29	0.13

*PEAK NORMALIZED AXIAL ENERGY FLUCTUATION

Figure 15. PPM Magnetic Field Results.

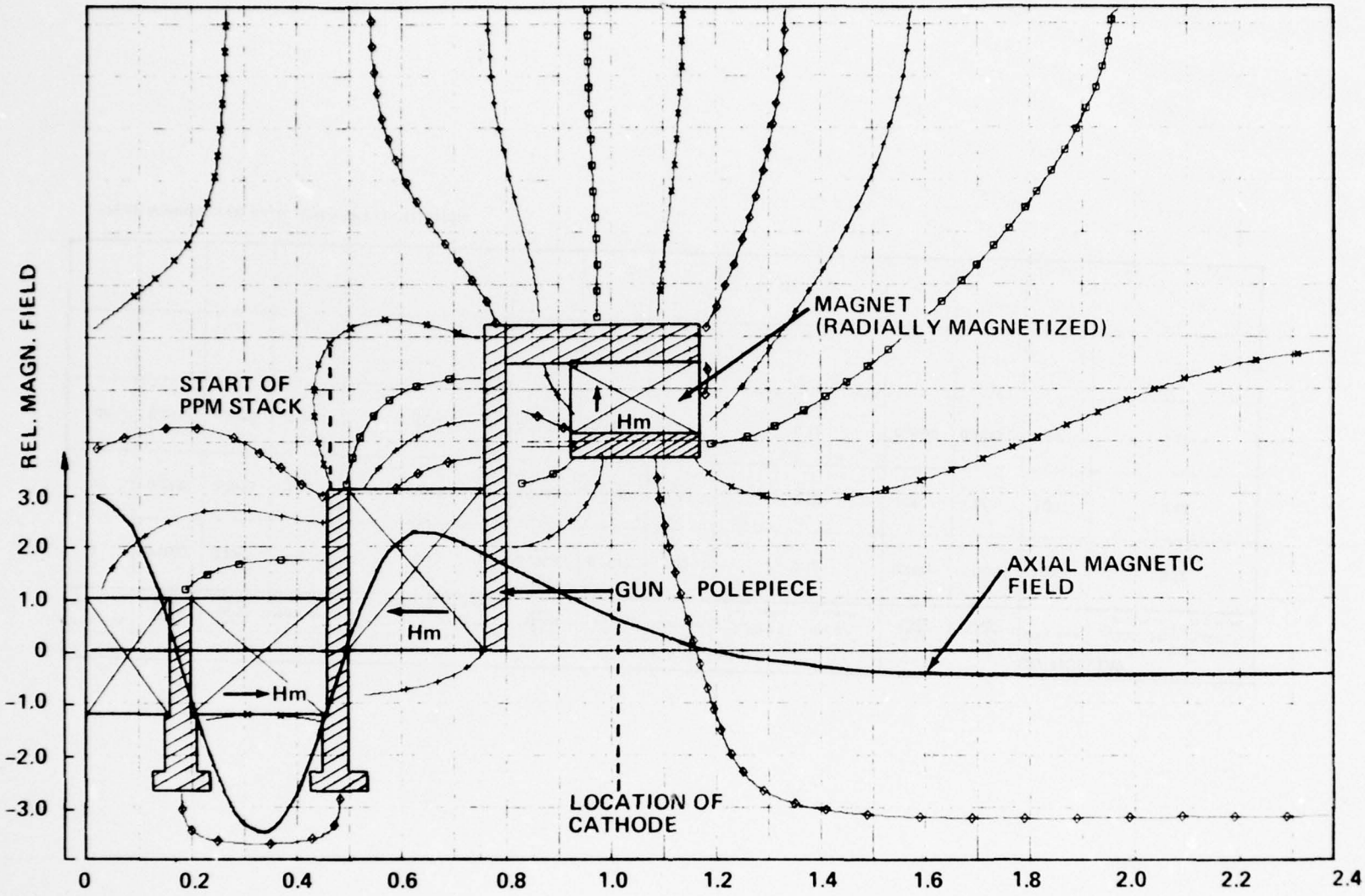

Figure 16. PPM Focusing System with Flux Threading of the Cathode.

5. GUN STRUCTURE, SOLID CW BEAM

There were no real problems in fabrication and assembly of the gun structure. As mentioned previously, the gun is a non-intercepting gridded gun. The gun contains two sets of grids with a transparency of 80 percent. The grid closest to the cathode operates at cathode potential and prevents electron emission from areas of the cathode covered by the grid vanes of both grids. The second grid is used for control of the beam current.

The first grid was placed directly in contact with the cathode and is operating at approximately cathode temperature. This eliminates the assembly problems associated with the close spacing between the cathode and shadow grid in the conventional non-intercepting gun. In addition, a significant improvement is obtained in the electron optical performance of the gun because the focusing grid operates at close to cathode temperature. Since electron emission must be inhibited from the grid vanes, the focus grid was coated with a thin layer of zirconium to inhibit grid emission.

6. BEAM ANALYZER TESTS

6.1 ELECTROSTATIC BEAM

The gun with the single control grid that produces a solid low-current mode beam was tested in the beam analyzer under electrostatic conditions. The results of the tests are shown in Figure 17 through 20. The results are in fairly good agreement with the computer analysis. The beam analyzer showed a laminar beam profile with a minimum beam diameter in the high-current mode of 0.132 in (the desired beam diameter is 0.130 in). Grid interception in the pulse mode, with 220 volts applied to the grid was 3.6 mA., corresponding to 0.3 percent grid interception.

The beam was also studied at microperveance of 0.3, corresponding to a ratio in power of 10:1. As excepted, the ratio between the two electrostatic beam diameters was great. This perveance will also be examined with magnetic field after a small adjustment in the magnetic field is made.

6.2 CONFINED FLOW BEAM

The first test of the gun producing a solid low current mode beam was completed. A spiraling of the beam was experienced, due to localized saturation of the iron polepiece outside the gun envelope by the radially magnetized Samarium cobalt magnet. This magnet consists of six radially magnetized segments and is used for the proper shaping of the magnetic field in the gun region. The strength of this magnet is adjusted by varying the number of the segments. It turned out that only one segment was needed to obtain the correct field variation on the axis. The polepiece saturated in the vicinity of the magnet producing large asymmetry in the magnetic field, causing the electron beam to spiral. A new design of the magnetic circuit surrounding the gun with an improved polepiece was designed and fabricated and the beam analyzer tests will be resumed.

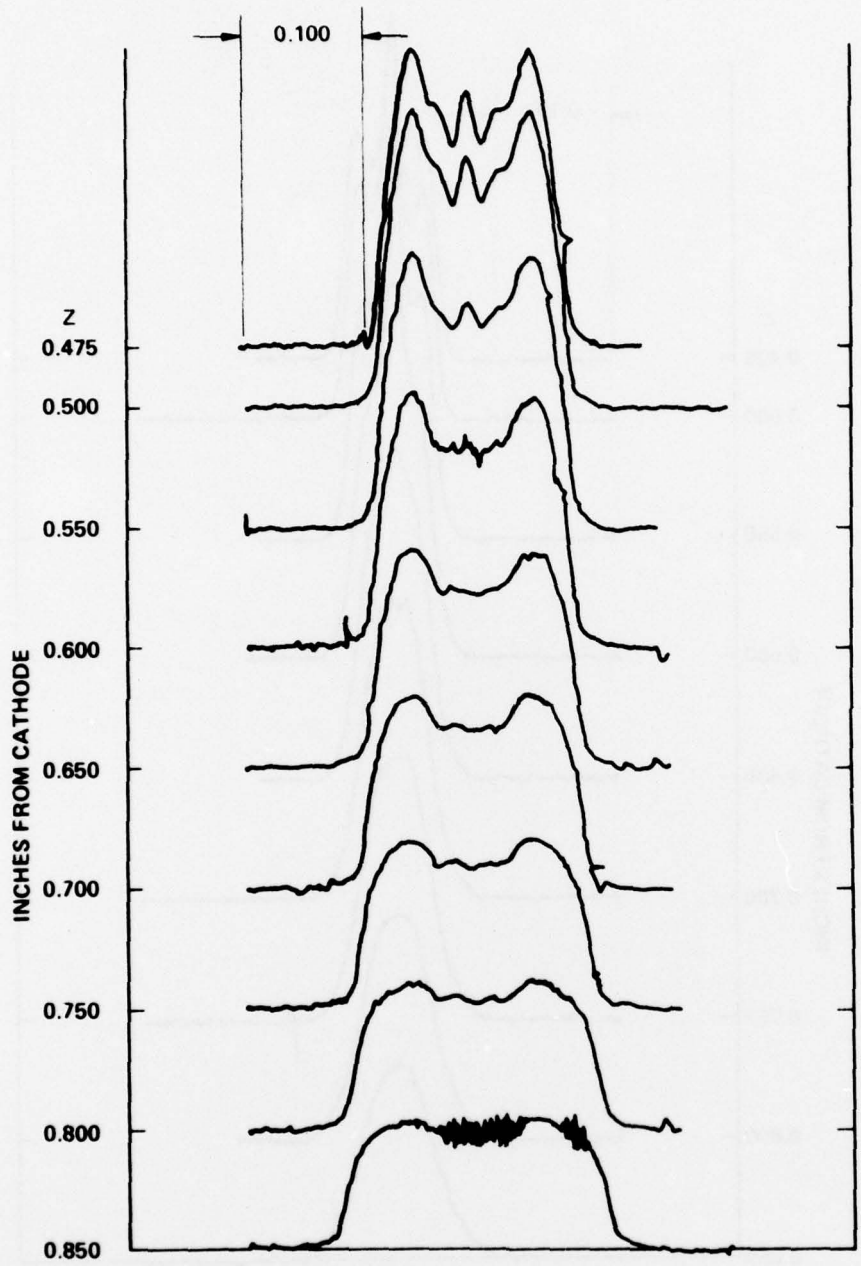

Figure 17. Beam Analyzer Result of Electrostatic Beam - High-Current Mode ($\mu k = 1.5$).

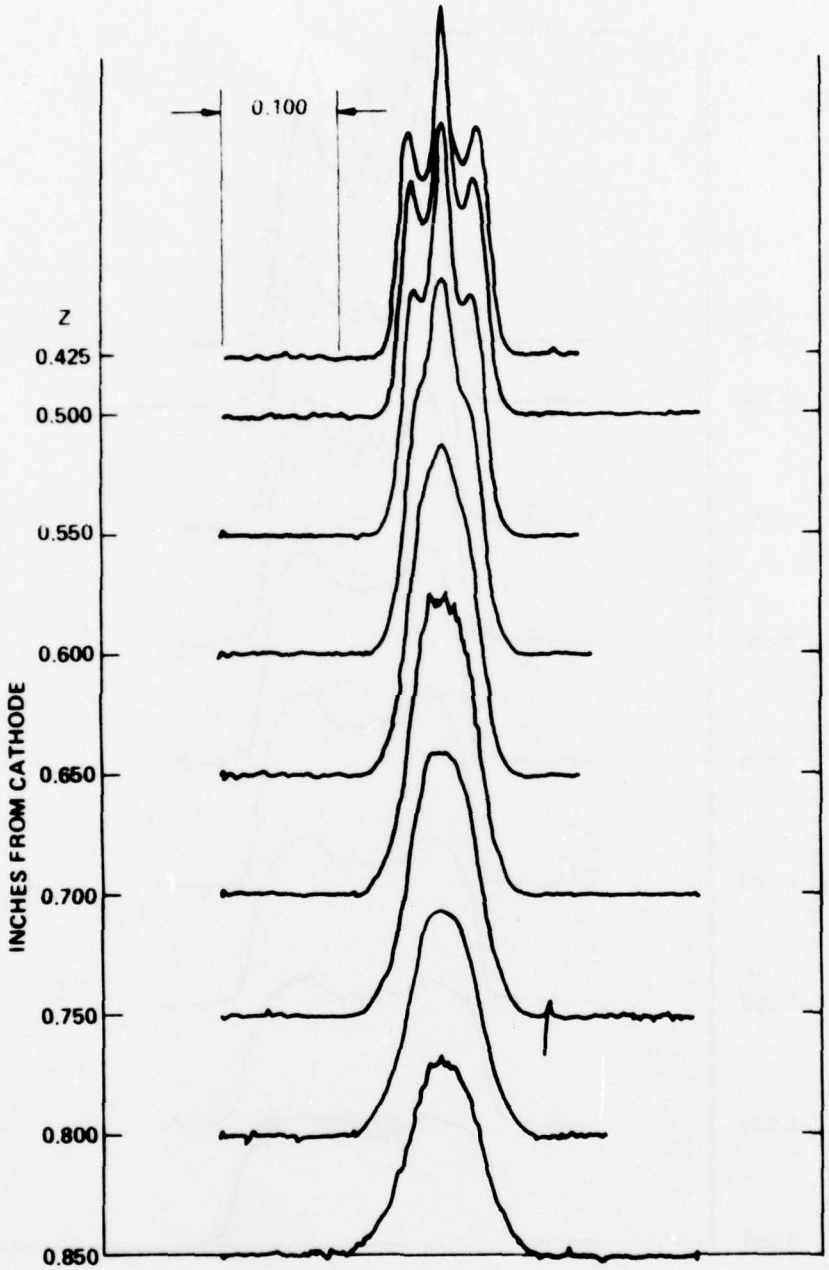

Figure 18. Beam Analyzer Result of Electrostatic Beam Low-Current Mode ($\mu k = 0.5$).

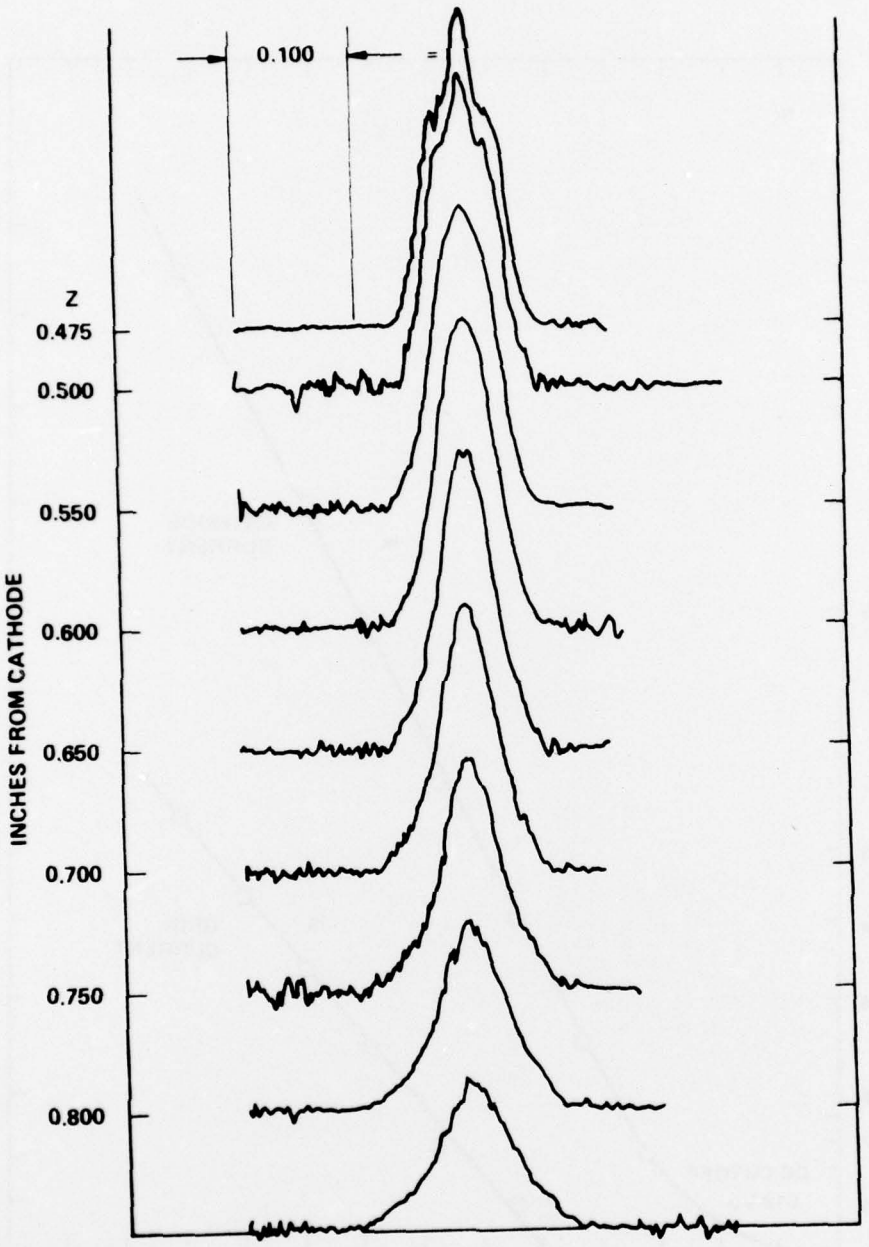

Figure 19. Beam Analyzer Result of Electrostatic Beam Low-Current Mode ($\mu k = 0.3$).

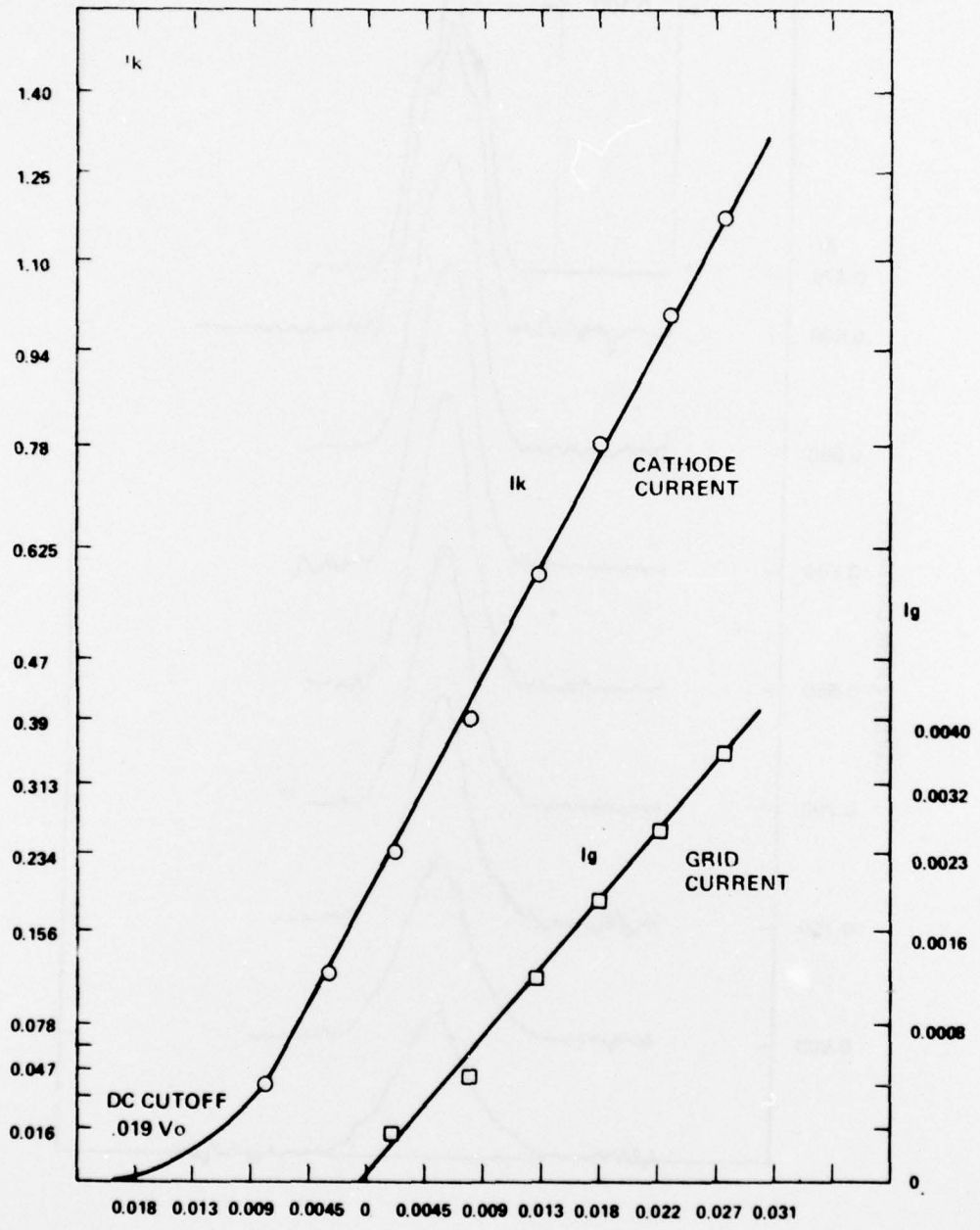

Figure 20. Cutoff Characteristics, Normalized Cathode and Grid Current vs Normalized Grid Voltage.

APPENDIX A

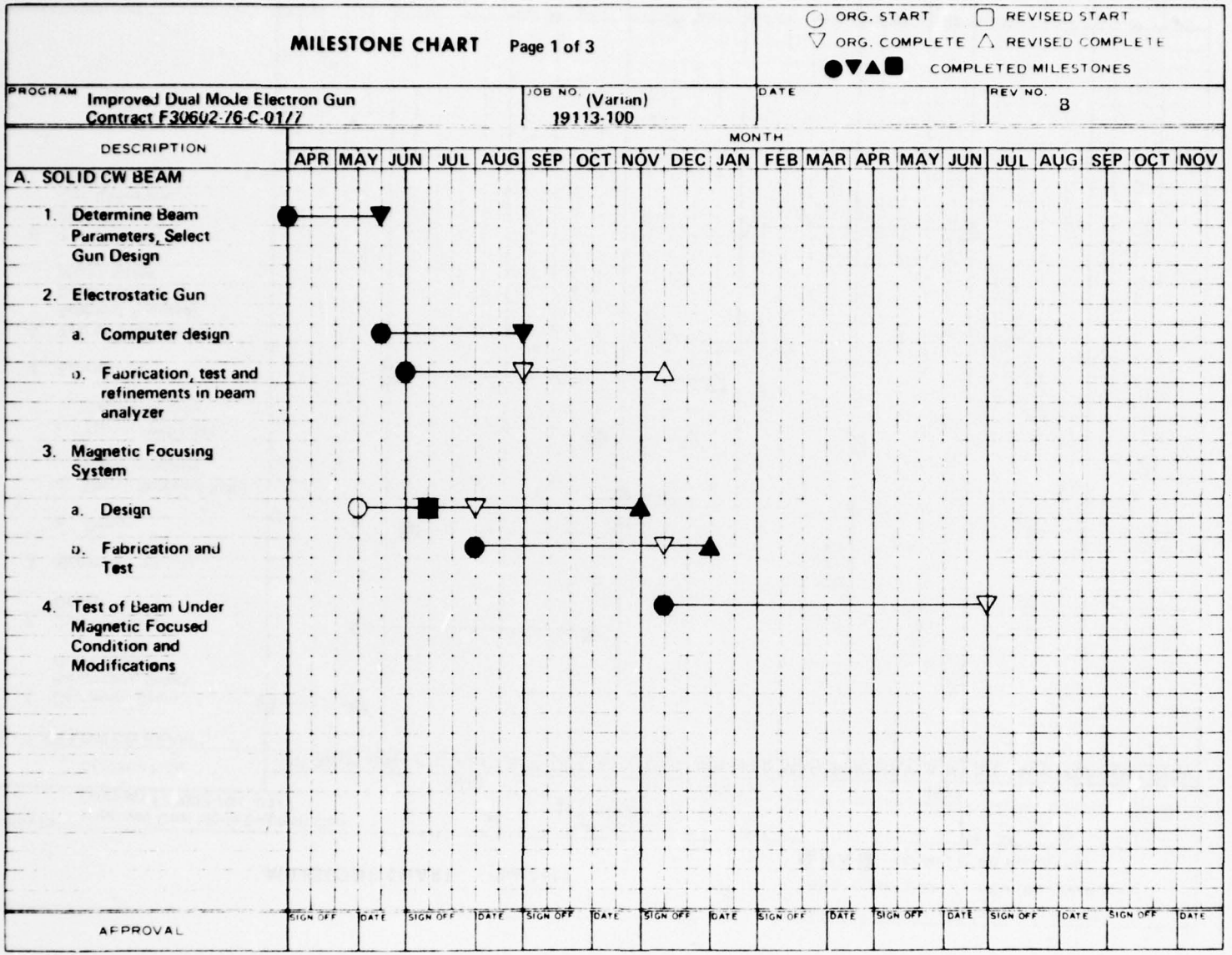
MILESTONE CHART Page 1 of 3
ORG. START
REVISED START
ORG. COMPLETE
REVISED COMPLETE
COMPLETED MILESTONES
PROGRAM
Improved Dual Mode Electron Gun
Contract F30602-76-C-0177
JOB NO.
(Varian)
19113-100
DATE
REV NO.
8
DESCRIPTION
MONTH
APR MAY JUN JUL AUG SEP OCT NOV DEC JAN FEB MAR APR MAY JUN JUL AUG SEP OCT NOV
A. SOLID CW BEAM
1. Determine Beam Parameters, Select Gun Design
2. Electrostatic Gun
a. Computer design
b. Fabrication, test and refinements in beam analyzer
3. Magnetic Focusing System
a. Design
b. Fabrication and Test
4. Test of Beam Under Magnetic Focused Condition and Modifications
APPROVAL
SIGN OFF
DATE

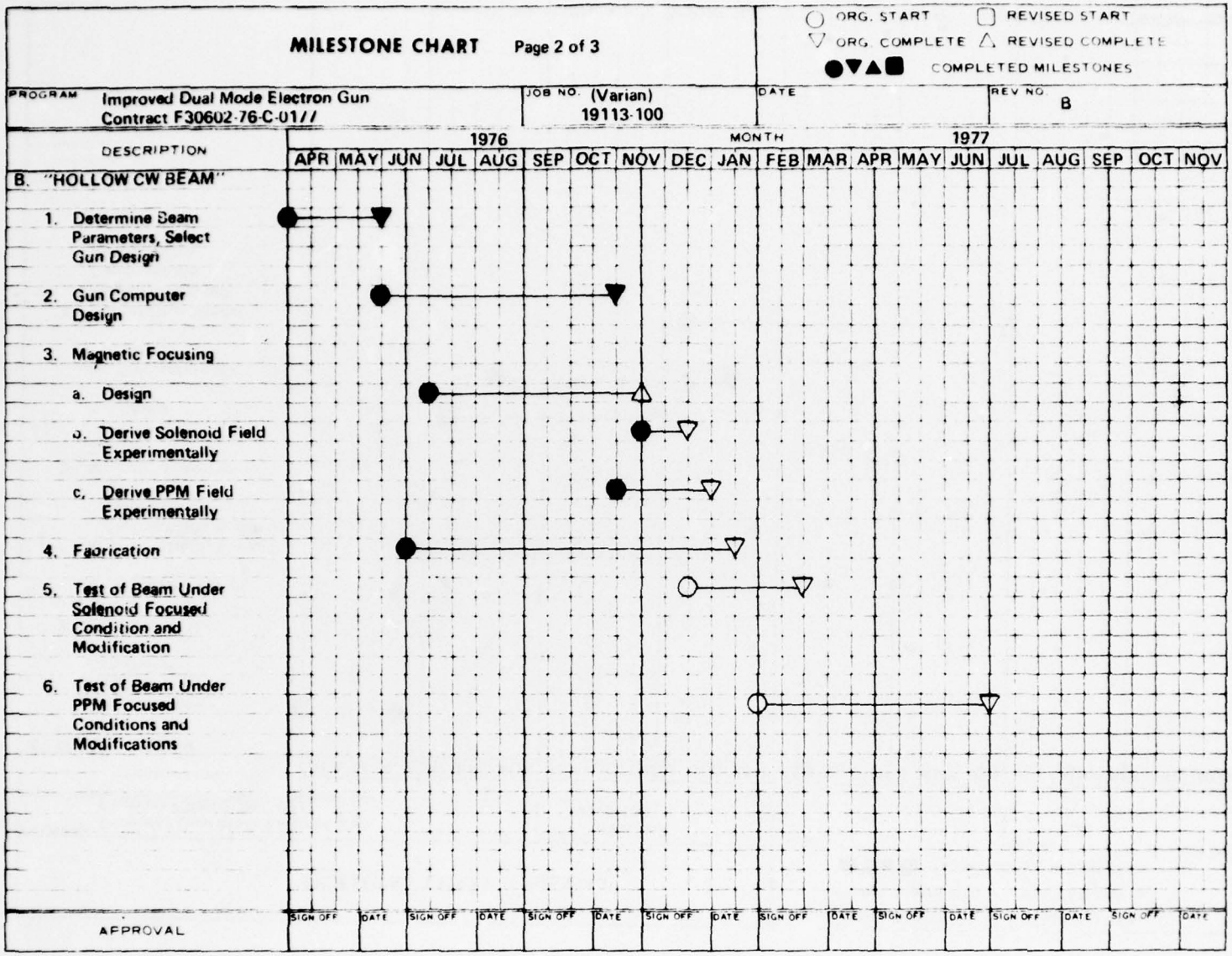
MILESTONE CHART Page 2 of 3
ORG. START
REVISED START
ORG. COMPLETE
REVISED COMPLETE
COMPLETED MILESTONES
PROGRAM Improved Dual Mode Electron Gun Contract F30602-76-C-0111
JOB NO. (Varian) 19113-100
DATE
REV NO B
DESCRIPTION
MONTH
1976
1977
APR MAY JUN JUL AUG SEP OCT NOV DEC JAN FEB MAR APR MAY JUN JUL AUG SEP OCT NOV
B. "HOLLOW CW BEAM"
1. Determine Beam Parameters, Select Gun Design
2. Gun Computer Design
3. Magnetic Focusing
a. Design
b. Derive Solenoid Field Experimentally
c. Derive PPM Field Experimentally
4. Fabrication
5. Test of Beam Under Solenoid Focused Condition and Modification
6. Test of Beam Under PPM Focused Conditions and Modifications
APPROVAL
SIGN OFF
DATE

MILESTONE CHART Page 3 of 3

○ ORG. START ⌷ REVISED START
▽ ORG. COMPLETE △ REVISED COMPLETE
●▼▲■ COMPLETED MILESTONES

PROGRAM: Improved Dual Mode Electron Gun Contract F30602-76-C-0177
JOB NO.: (Varian) 19113-100
DATE:
REV NO: B

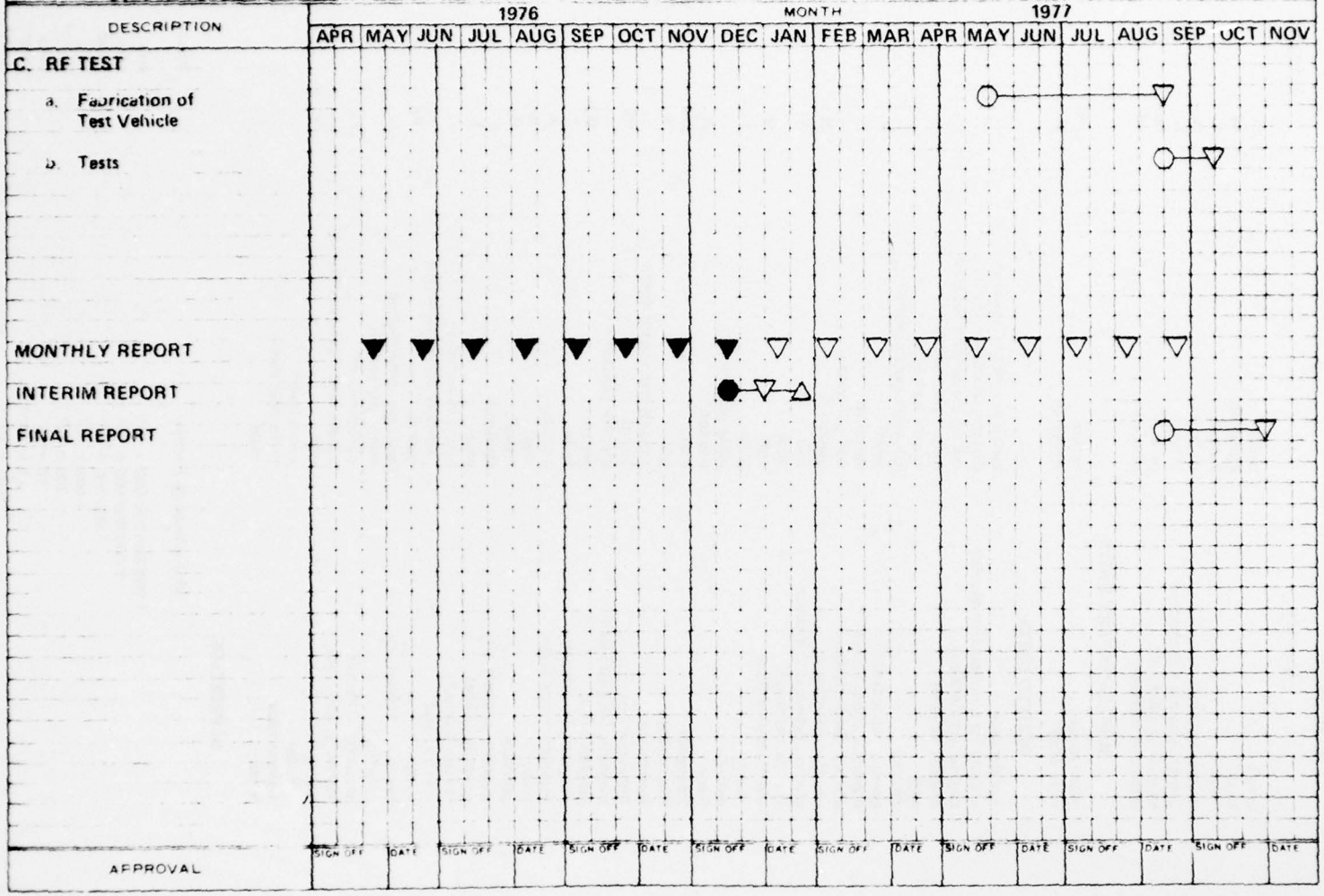

METRIC SYSTEM

BASE UNITS:

Quantity	Unit	SI Symbol	Formula
length	metre	m	...
mass	kilogram	kg	...
time	second	s	...
electric current	ampere	A	...
thermodynamic temperature	kelvin	K	...
amount of substance	mole	mol	...
luminous intensity	candela	cd	...

SUPPLEMENTARY UNITS:

plane angle	radian	rad	...
solid angle	steradian	sr	...

DERIVED UNITS:

Acceleration	metre per second squared	...	m/s
activity (of a radioactive source)	disintegration per second	...	(disintegration)/s
angular acceleration	radian per second squared	...	rad/s
angular velocity	radian per second	...	rad/s
area	square metre	...	m
density	kilogram per cubic metre	...	kg/m
electric capacitance	farad	F	A·s/V
electrical conductance	siemens	S	A/V
electric field strength	volt per metre	...	V/m
electric inductance	henry	H	V·s/A
electric potential difference	volt	V	W/A
electric resistance	ohm		V/A
electromotive force	volt	V	W/A
energy	joule	J	N·m
entropy	joule per kelvin	...	J/K
force	newton	N	kg·m/s
frequency	hertz	Hz	(cycle)/s
illuminance	lux	lx	lm/m
luminance	candela per square metre	...	cd/m
luminous flux	lumen	lm	cd·sr
magnetic field strength	ampere per metre	...	A/m
magnetic flux	weber	Wb	V·s
magnetic flux density	tesla	T	Wb/m
magnetomotive force	ampere	A	...
power	watt	W	J/s
pressure	pascal	Pa	N/m
quantity of electricity	coulomb	C	A·s
quantity of heat	joule	J	N·m
radiant intensity	watt per steradian	...	W/sr
specific heat	joule per kilogram-kelvin	...	J/kg·K
stress	pascal	Pa	N/m
thermal conductivity	watt per metre-kelvin	...	W/m·K
velocity	metre per second	...	m/s
viscosity, dynamic	pascal-second	...	Pa·s
viscosity, kinematic	square metre per second	...	m/s
voltage	volt	V	W/A
volume	cubic metre	...	m
wavenumber	reciprocal metre	...	(wave)/m
work	joule	J	N·m

SI PREFIXES:

Multiplication Factors	Prefix	SI Symbol
1 000 000 000 000 = 10^{12}	tera	T
1 000 000 000 = 10^{9}	giga	G
1 000 000 = 10^{6}	mega	M
1 000 = 10^{3}	kilo	k
100 = 10^{2}	hecto*	h
10 = 10^{1}	deka*	da
0.1 = 10^{-1}	deci*	d
0.01 = 10^{-2}	centi*	c
0.001 = 10^{-3}	milli	m
0.000 001 = 10^{-6}	micro	μ
0.000 000 001 = 10^{-9}	nano	n
0.000 000 000 001 = 10^{-12}	pico	p
0.000 000 000 000 001 = 10^{-15}	femto	f
0.000 000 000 000 000 001 = 10^{-18}	atto	a

* To be avoided where possible.

MISSION
of
Rome Air Development Center

RADC plans and conducts research, exploratory and advanced development programs in command, control, and communications (C^3) activities, and in the C^3 areas of information sciences and intelligence. The principal technical mission areas are communications, electromagnetic guidance and control, surveillance of ground and aerospace objects, intelligence data collection and handling, information system technology, ionospheric propagation, solid state sciences, microwave physics and electronic reliability, maintainability and compatibility.